Biol Cybern (2009) 100:475–489
DOI 10.1007/s00422-009-0298-5

ORIGINAL PAPER

Biological Cybernetics

# Feedback-induced gain control in stochastic spiking networks

**Connie Sutherland · Brent Doiron · André Longtin**

Received: 16 September 2008 / Accepted: 5 February 2009 / Published online: 4 March 2009


**Abstract** The joint influence of recurrent feedback and noise on gain control in a network of globally coupled spiking leaky integrate-and-fire neurons is studied theoretically and numerically. The context of our work is the origin of divisive versus subtractive gain control, as mixtures of these effects are seen in a variety of experimental systems. We focus on changes in the slope of the mean firing frequency-versus-input bias ($f$–$I$) curve when the gain control signal to the cells comes from the cells' output spikes. Feedback spikes are modeled as alpha functions that produce an additive current in the current balance equation. For generality, they occur after a fixed minimum delay. We show that purely divisive gain control, i.e. changes in the slope of the $f$–$I$ curve, arises naturally with this additive negative or positive feedback, due to a linearizing actions of feedback. Negative feedback alone lowers the gain, accounting in particular for gain changes in weakly electric fish upon pharmacological opening of the feedback loop as reported by Bastian (J Neurosci 6:553–562, 1986). When negative feedback is sufficiently strong it further causes oscillatory firing patterns which produce irregularities in the $f$–$I$ curve. Small positive feedback alone increases the gain, but larger amounts cause abrupt jumps to higher firing frequencies. On the other hand, noise alone in open loop linearizes the $f$–$I$ curve around threshold, and produces mixtures of divisive and subtractive gain control. With both noise and feedback, the combined gain control schemes produce a primarily divisive gain control shift, indicating the robustness of feedback gain control in stochastic networks. Similar results are found when the "input" parameter is the contrast of a time-varying signal rather than the bias current. Theoretical results are derived relating the slope of the $f$–$I$ curve to feedback gain and noise strength. Good agreement with simulation results are found for inhibitory and excitatory feedback. Finally, divisive feedback is also found for conductance-based feedback (shunting or excitatory) with and without noise.

**Keywords** Gain control · Feedback · Noise · Leaky integrate-and-fire · Electric fish · Spiking networks · Delays

## 1 Introduction

There is a long standing interest in the mapping from presynaptic input rates to postsynaptic firing rates (Segundo 1970; Perkel et al. 1964). In many situations the brain performs a scaling operation on the neural response to input. For instance, gaze direction scales the response strength in primary visual (Trotter and Celebrini 1999) and posterior parietal cortex (Andersen and Mountcastle 1983; Salinas and Abbott 1996). Contrast invariance of receptive field properties (Alitto and Usrey 2004) and orientation selectivity (Ferster and Miller 2000) requires a contrast dependent scaling of responses in primary visual cortex. Subject attention sets the response gain of cells in primary visual cortex (McAdams and Reid 2005), as well as in V4 (McAdams and Maunsell 1999). Response scaling is measured by the

This article is part of a special issue on Neuronal Dynamics of Sensory Coding.

C. Sutherland · B. Doiron · A. Longtin (✉)
Center for Neural Dynamics, University of Ottawa,
150 Louis Pasteur, Ottawa K1N 6N5, Canada
e-mail: alongtin@uottawa.ca

C. Sutherland · B. Doiron · A. Longtin
Department of Physics, University of Ottawa,
150 Louis Pasteur, Ottawa K1N 6N5, Canada

B. Doiron
Department of Mathematics, University of Pittsburgh,
Pittsburgh 15260, USA

changes in the frequency-versus-input current ($f$–$I$) characteristic of a cell. More specifically, the neuronal *gain* describes the sensitivity of the output firing frequency in response to changes in the strength of the stimulus input. Many studies have shown that gain control can be an important computational tool in the central nervous system (Douglas et al. 1995; Salinas and Thier 2000) and subsequent references therein).

Gain sensitivity has been characterized in a large number of experimental and modeling studies, most often as the slope of the $f$–$I$ characteristic. If the slope of this $f$–$I$ curve is high, a small range in input current is mapped by the cell into a larger variation in instantaneous firing rate. Conversely, a small gain serves to limit the range of firing rates that stimuli can produce, thereby scaling down the influence of the input on the output. This picture of a static $f$–$I$ curve performing an input–output operation holds as long as the input signal fluctuations are slow compared to the membrane time constant; in this case the cell adjusts its firing rate to the current signal (see Ly and Doiron 2009 for a discussion of gain control for non-stationary responses). The membrane time constant, which governs the input resistance and reflects the complement of conductances present in the cell, along with membrane fluctuations in the cell, are the main determinants of the gain of a single cell in isolation.

Gain control mechanisms alter a neuron's $f$–$I$ curve. Figure 1 shows several schematic examples of common gain manipulations, and in the next few sections we list specific cases from the literature where such gain manipulations are reported. From a neuro-computational perspective, divisive gain manipulation (Fig. 1b) is often assumed in rate-based models of neurons (Carandini and Heeger 1994; Chance and Abbott 2000), and is a central feature in both visual and motor control (Salinas and Thier 2000). However, biophysical mechanisms for divisive gain control have been elusive (Holt and Koch 1997; Chance et al. 2002). Our paper details how divisive gain control arises naturally with feedback, with or without noise. To give context to feedback-induced divisive gain control we first review past gain control mechanisms.

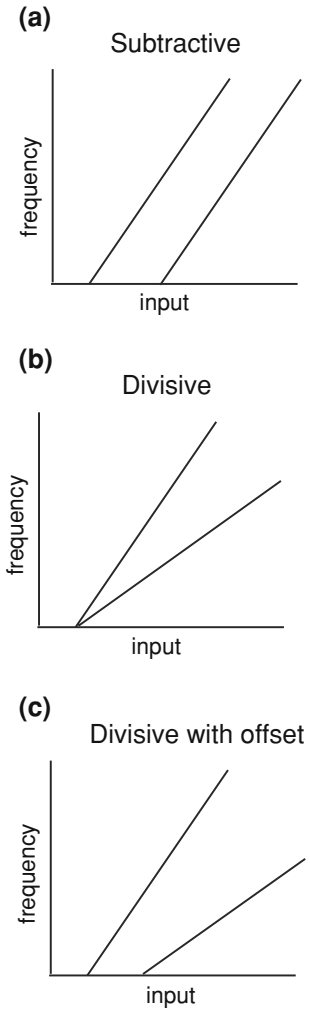


**Fig. 1** Schematic description of various types of gain modulation. **a** A subtractive gain modulation preserves the slope of the transfer curve yet shifts the onset of firing. This occurs for a shift in the leak conductance (Holt and Koch 1997; Chance et al. 2002; Mehaffey et al. 2005). **b** 'Pure' divisive gain modulation reduces the slope of the transfer function yet preserves the onset of firing. Known mechanisms include balanced conductance fluctuations in the input conductance (Chance et al. 2002), inhibition of the dendrite in deterministic spiking systems (Mehaffey et al. 2005), recurrent connectivity in neural populations (Douglas et al. 1995), and spike frequency adaptation (Ermentrout 1998). **c** Divisive modulation with an offset, or rheobase, shift occurs when an unbalanced conductance-based fluctuations combine the mechanisms in **a** and **b** (Doiron et al. 2001; Chance et al. 2002)

### 1.1 Gain control with stochastic shunting inhibition

One commonly assumed fast-acting mechanism of gain control is shunting inhibition, i.e. through a large amplitude conductance $G_s$ with a reversal potential $V_s$ near the resting potential $V_r$ of the cell. Even though $G_s$ is large, since $V_s \approx V_r$, the current $I_s = G_s(V - V_s)$ contributed will be small. The main effect of this inhibition, classically mediated by $GABA_A$ type channels, is through the reduction of the input resistance and thus of the membrane time constant $\tau$. This decreases the effect of excitatory input, whether due to an injected current input or to synaptic input. This form of divisive rate control is often assumed in rate formulations of firing in neural networks (Chance and Abbott 2000). The hope that this would follow naturally for more realistic spiking neurons was guided by the fact that membrane voltage does relate to input current in a divisive manner in the subthreshold regime (i.e. the regime where no spikes occur). This is simply Ohm's law: the slope of the $V$–$I$ curve is the reciprocal of the total conductance. Thus, it was expected that shunting inhibition would lead to a divisive gain manipulation of the $f$–$I$ curve (Fig. 1b). However, Holt and Koch

(1997) showed that this subthreshold divisive gain control gives way to subtractive gain control (Fig. 1a) in the suprathreshold firing regime. This is a consequence of the resetting of the voltage following spikes, which qualitatively alters the relation between voltages and currents averaged over short times. They showed this effect in both a reconstructed visual pyramidal cell model and its simplified leaky integrate-and-fire (LIF) version. Note that the context here is that the inhibition is independent of the firing of the cell.

One can obtain divisive effects with (Fig. 1c) or without (Fig. 1b) subtractive effects when the noise intrinsic to a cell and/or associated with synaptic inputs, is taken into account (Doiron et al. 2001; Chance et al. 2002; Longtin et al. 2002; Prescott and De Koninck 2003). Our original study (Doiron et al. 2001) was based on a compartmental ionic model built from anatomical and physiological data from a pyramidal cell of the electrosensory lateral line lobe of the weakly electric fish *Apteronotus leptorhynchus*. The simple inclusion of noise in the gain control problem thus revealed a mechanism for divisive gain control at the single cell level in a feedforward configuration. The noise arose naturally from simulations of the feedforward inhibitory synaptic input on the compartmental model using the program NEURON, since pre-synaptic spike trains had Poisson statistics. In other words, the variance of the point process associated with the inhibition increased in proportion with the mean frequency of inhibitory inputs. This effect was then replicated in a simpler integrate-and-fire version of the ionic model:

$$C\frac{\mathrm{d}V}{\mathrm{d}t} = -\left[\overline{g} + \sigma(\overline{g})\eta(t)\right]V + I \tag{1}$$

where $\eta(t)$ was lowpass-filtered Gaussian white noise added to the mean conductance $\overline{g}$, meant to represent the mean total inhibitory input in the compartmental model. The noise on the total conductance was necessary to obtain sigmoidally increasing $f$–$I$ curves near rheobase, as seen experimentally and in the compartmental model. $f$–$I$ curves for increasing mean levels of inhibition $\overline{g}$ simply shifted rightwards (as in Holt and Koch 1997) if the noise intensity $\sigma^2$ was independent of the mean inhibition, i.e. subtractive gain control occurred. However, if $\sigma^2$ was increased monotonically with $\overline{g}$, as expected for Poisson statistics, divisive gain control was observed at lower frequencies, with subtractive behavior at higher frequencies. Further, purely divisive gain control is possible if a balanced state of feedforward excitation and inhibition exists (Chance et al. 2002). The question then arises about the consequences of feedback instead of feedforward, which is our focus below.

In fact, the role of noise, intrinsic or from synaptic inputs, has a long history (Lindner et al. 2004). It has been implicated in the linearization of $f$–$I$ curves, smoothing of responses via e.g. elimination of phase locking (Perkel et al. 1964; Knight 1972; French et al. 1972), and amplification of slow or fast subthreshold input via stochastic resonance (Longtin 1993). Input fluctuations are thought to be critical in the contrast invariance of orientation tuning in primary visual cortex (Anderson et al. 2000; Hansel and van Vreeswijk 2002). Further, the impact of conductance (Burkitt et al. 2003; Mitchell and Silver 2003; Prescott and De Koninck 2003) and current (Higgs et al. 2007; Arsiero et al. 2007) fluctuations on response gain continues to be a subject of great interest.

### 1.2 Divisive control with adaptation and feedback

The role that feedback plays on gain control has also received attention (Diez-Martinez and Segundo 1983). In many systems, and in sensory systems in particular, *excitation or inhibition actually arise from the activity of the neurons whose gain is under investigation.* Divisive gain control (Fig. 1b) does occur in simple rate models of neurons with recurrent feedback, a property that has lead to many studies of neural multiplication (see, e.g. Salinas and Abbott (1996) in the visual gain fields context), or of gain control via shunting inhibition and possible effects on network response time in rate-based neural networks, both feedforward and recurrent (Douglas et al. 1995; Chance and Abbott 2000). Other results showing divisive effects owing to recurrent activity also exist across the spiking neuron literature in the context of synchronization (White et al. 1998; Pauluis et al. 1999; Le Masson et al. 2002), lateral inhibition (Arevian et al. 2007), and autaptic inhibition (Bacci et al. 2003).

In particular, the computational study of Douglas et al. (1995) showed that divisive behavior is possible in conductance-based recurrent models. They performed an analysis using a scenario where firing rate is proportional to membrane voltage which is in turn inversely proportional to the amount of conductance (both intrinsic, and from recurrent synaptic connections). They also show the effect numerically in a recurrent network of conductance-based spiking pyramidal cells and interneurons. Their numerics show that input noise is suppressed by the network. Our study of divisive control is motivated in part by the fact that Douglas et al. (1995) tacitly assumed a simple relationship between membrane voltage and output firing. Given the caveats later raised by Holt and Koch (1997) about such an assumption (discussed above), and by the need for matching theory and numerics with networks stochastic neurons, we revisit the feedback induced gain control originally proposed by Douglas et al. (1995).

Adaptation currents, typically either voltage (Brown and Adams 1980) or calcium (Madison and Nicoll 1984) dependent potassium currents, are also a form of feedback that is internal to the cell. Adaptation requires (and follows) spiking, but does not require self-feedback mediated by axonal collaterals (autapses) or feedback from other populations. The theoretical effect of adaptation on $f$–$I$ curves was first

studied by Ermentrout (1998). He showed that adaptation causes a linearization of the $f$–$I$ curve; while the analysis was limited to suprathreshold signals, the numerics indicated that the effect was also present in the whole peri-threshold regime as well. We will show below that his analysis contains the root of the divisive gain control via feedback which we emphasize in our paper. Related 'internal' divisive gain control schemes can occur through synaptic manipulation of active dendrites in weakly electric fish (Mehaffey et al. 2005), layer 5 pyramidal neurons (Larkum et al. 2004), and looming sensitive neurons in locust (Gabbiani et al. 2002).

### 1.3 Gain control with feedback and noise

Given the strong influence that noise and feedback separately have on gain, the time is ripe to analyze more thoroughly the simultaneous effect of feedback and noise. Our paper is thus first and foremost concerned with gain changes when spiking feedback is present, and what role noise, both internal to the neurons or external to the network, plays in such feedback mediated gain control. For generality, we include feedback delays in our analysis, to account for the finite time of response to feedback currents when they arise from another neuron population. In principle we are interested in the more biophysically realistic spiking dynamics; however while. We expect our focus is on leaky integrate-and-fire dynamics for our simulations and theory. We expect our results generalize to other firing dynamics such as quadratic integrate-and-fire, and Hodgkin–Huxley dynamics as well.

The motivation for our work on feedback gain control is drawn mainly from experiments on weakly electric fish, although experimental examples of neural gain control are ubiquitous. The primary receptors, known as electroreceptors, project to pyramidal cells of the electrosensory lateral line lobe (ELL). These in turn excite higher brain nuclei, which in turn project back to the ELL. The projections are of mixed polarity: the activity from higher brain excites the ELL and also inhibits it via interneurons. It is natural to think that, to first order, this feedback implements some form of gain control. In vivo studies in the weakly electric fish have shown that feedback can divisively alter the $f$–$I$ curve to reduce the frequency response range of the ELL (Bastian 1986) and in this way adapt to stimuli. Figure 2 shows the change in mean firing rate as the feedback from the cerebellar structure known as the EGP is opened in vivo. One sees a change in slope, with relatively little change at rheobase—although one may argue a small leftward shift of rheobase as the feedback is opened (Fig. 1c), but more statistical analysis may be needed to firmly establish this small effect. It is thus clear that the feedback acts in a divisive inhibitory fashion. More recent experimental results on lateral inhibition (Arevian et al. 2007) and autaptic inhibition (Bacci et al. 2003) further motivate our study.

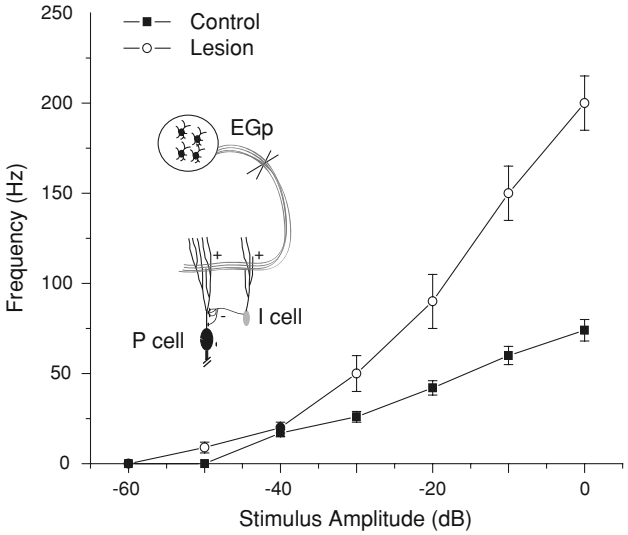


**Fig. 2** Change in firing rate with respect to baseline firing rate as a function of stimulus amplitude from in vivo measurements on a pyramidal cell in the electrosensory lateral line lobe of the electric fish *Apteronotus leptorhynchus*. In the control case (*black squares*) the feedback from the cerebellar structure known as the EGP is intact. The main effect of removing the feedback from the parallel fibers (opening the feedback loop) is an increase in slope, which implies that the net polarity of the feedback is inhibitory. Data are redrawn from Bastian (1986) (see also Mehaffey et al. 2005)

Nelson (1994) studied how feedback could work in the electric fish by focussing on the neuron transmembrane potential as the quantity fed back to itself, rather than the firing rate. His study enabled the understanding of filtering properties that can arise from the feedback and how, with both excitatory and inhibitory components, the filtering could be set independently of the firing rate of the cell. Given the results of Holt and Koch (1997), it is also natural to extend this study to more realistic spiking networks where spike trains are being fed back. One goal of our study is thus to see how the feedback-mediated gain control in the electrosensory system (Bastian 1986) can arise from a realistic spiking network.

In the next section, we present the model feedback network of stochastic spiking neurons used in our study. Results are presented in Sect. 3. Section 4 develops the theory applicable to that network. Comparisons between theory and simulation results are the subject of Sect. 5. A discussion of the results along with suggestions of future research directions follows in Section 6.

## 2 Model

The neural network we consider consists of $N$ identical stochastic leaky integrate-and-fire neurons connected by delayed global feedback. $V_i$ represents the membrane potential of the $i$th neuron in the network. A given neuron $i$

fires at time $t_{ij}$ whenever its voltage reaches a fixed threshold $\theta = 1$ from below. Immediately after this time, the voltage $V_i$ is reset to zero. Spikes have a minimal separation due to the absolute refractory period $\tau_R$ chosen equal to 0.1. As in Doiron et al. (2004), each of the neurons evolves according to

$$\frac{dV_i}{dt} = -V_i + \eta_i(t) + I_{\text{ext}i}(t) + g\sum_k^N K_{\tau_d} * x_k(t) \tag{2}$$

where

$$I_{\text{ext}i}(t) = \mu + \sigma\xi_i(t) \tag{3}$$

$$K_{\tau_d} * x(t) = \int_{\tau_d}^{\infty} d\tau x(t-\tau)\alpha^2(\tau-\tau_d)e^{-\alpha(\tau-\tau_d)}. \tag{4}$$

Each neuron has its own internal noise, $\eta_i(t)$, modeled by zero-mean Gaussian white noise with correlation function $\langle\eta_m(t)\eta_n(t')\rangle = 2D_{\text{int}}\delta(t-t')\delta_{mn}$ where $\delta(t-t')$ is the Dirac delta function and $\delta_{mn}$ is the Kronecker delta. We will refer to $D_{\text{int}}$ as the internal noise intensity. The external input current to the network consists of an average input bias, $\mu$, which is the same for all cells, and a time-varying input, $I_{\text{ext}i}(t)$, which is modeled by another zero-mean Gaussian white noise $\xi_i(t)$. For simplicity we assume that this component of external noise is global, i.e. $\xi_i(t) \equiv \xi(t)$. The intensity of $I_{\text{ext}i}(t)$ is dependent upon the associated intensity of the time-varying input $\sigma^2$. The variance of the total noise for each cell is then the sum of the individual variances of $\eta_i$ and $\xi_i$.

The last term in Eq. (2) represents the delayed spatiotemporal feedback, where $x_k(t)$ is the output spike train (sequence of Dirac delta functions) of neuron $k$. Thus, when one neuron fires, every neuron (including the one that just fired) receives feedback current that begins after a fixed delay $\tau_d$. The time course of the current is determined by the convolution kernel $K_d$ (Doiron et al. 2004), with smoothing parameter $\alpha$. It is meant to mimic the smoothing properties of both the distal cells providing feedback as well as synaptic kinetics. A large value of $\alpha$ corresponds for example to rapid synaptic kinetics. Another way to look at the convolution kernel is that it mimics a distribution of feedback delays with a minimal delay $\tau_d$. In this formulation, the cells in the network are not connected directly to one another, but through the delayed feedback. This is a good approximation for the pyramidal cells of the ELL in weakly electric fish (Doiron et al. 2003; Berman and Maler 1999). These cells receive input from the primary sensory cells (electroreceptors) and feedback from higher brain structures such as the nucleus prae-eminentialis (Np). It is also a good approximation to certain parts of the feedback between the optic tectum and the nucleus isthmi in other animals (Brandt and Wessel 2007). Other systems may involve direct coupling between the cells in the same nucleus as well as more delayed input from distant nuclei (Schwabe et al. 2006). The gain control results in these cases are expected to be qualitatively similar to those below, except when delays due to travel of neural information to and from distant nuclei are sufficiently long that oscillatory activity ensues.

Time is scaled in units of the membrane time constant, and all firing rates are determined after transients had decayed. We consider negative feedback ($g < 0$) as well as positive feedback ($g > 0$) cases separately. Throughout we take $\tau_d = 1$. We are mainly interested in the mean firing rate of one cell in the network as a function of its bias $\mu$, i.e. its $f$–$I$ curve (where "I" is now $\mu$)—although we will also discuss how the rate varies with the variance (contrast) of the external noise. Because the network is homogeneous, all cells will have the same firing rate, which can thus be determined by averaging the firing activity per unit time over the whole network.

At larger delays and negative feedback, the firing rates in the network may oscillate, meaning that the spiking cells participate in a network oscillation. The network oscillation may also abruptly change its period, or its pattern (number of spikes per period) as the bias changes (Figs. 5–7), due to nonlinear phase locking effects caused by the feedback—the precise study of these effects is beyond the scope of our work. Also, the activity may be more or less synchronous, depending on the level of noise (generally more synchronous behavior with less noise). The simulation time at a given bias may not correspond to an integer number of periods of the steady state solution at that bias. This induces a small error in the estimation of the rate at larger delays and inhibitory strength. This error is minimized by using longer simulations, and is insignificant for the gain effects we are interested in. Nevertheless, these abrupt changes are most obvious in the jagged or wavy aspect of the $f$–$I$ curve for stronger inhibitory feedback, especially without noise (they are generally smoothed out by increasing noise). The firing rates will thus show an increasing trend as a function of bias, with fluctuations around this trend due to the abrupt changes and to the uneven sampling of the network oscillation.

## 3 Gain control with fluctuations and feedback

### 3.1 Noise-induced divisive gain control in the absence of feedback

The mean firing rate, or "activity", of a single neuron in the network without feedback is computed from numerical simulations and plotted against input bias $\mu$ (the average input current) in Fig. 3. This figure shows that, as noise intensity is increased, the gain increases for input biases in the subthreshold regime ($\mu < 1$ in this case), going from zero slope (deterministic neuron) to a finite slope (noise-driven neuron). At higher noise this slope will begin decreasing again (not

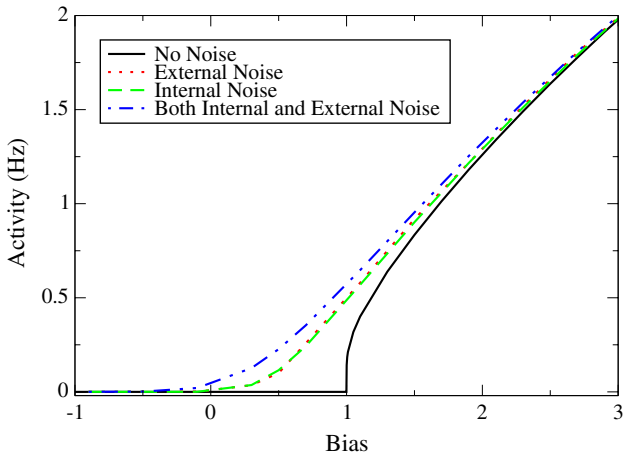


**Fig. 3** Mean firing rate $f$ versus input bias $I$ for one leaky integrate-and-fire neuron for increasing intensity of noise (see Eq. 2). No feedback is present ($g = 0$). For the zero-noise condition (*solid line*), we set both noise intensities to zero (external: $\sigma^2 = 0$ and internal: $D_{\text{int}} = 0$). Spiking occurs only for biases greater than 1. For the internal noise condition (*dashed line*), $D_{\text{int}} = 0.08$ and $\sigma^2 = 0$. For the external noise condition (*dotted line*), $\sigma^2 = 0.16$ and $D_{\text{int}} = 0$. With both internal and external noise, $\sigma^2 = 0.16$ and $D_{\text{int}} = 0.08$. Time is scaled in units of the membrane time constant (approximately 6 ms in the case of ELL pyramical cells), thus 1 Hz corresponds to one spike in 6 ms. As the amount of noise in the system increases the $f$–$I$ curve becomes more linear, i.e. the threshold nonlinearity is smoothed. This is due to noise-induced firing, which is especially visible below the deterministic threshold

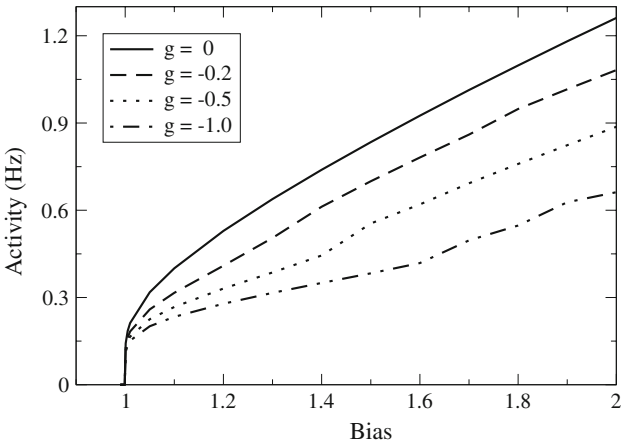


**Fig. 4** $f$–$I$ curves with increasing inhibitory feedback strength for a network of $N = 100$ neurons without noise. As the strength of inhibitory feedback is increased the $f$–$I$ curves divisively shift downward. Other parameters used in the simulation are as in Fig. 3. Note that the range of biases differs slightly from that used in Fig. 3 and $\alpha = 2$

shown—this is relevant to the low frequency limit of stochastic resonance—see Longtin (2000) and Lindner et al. 2004). A slight reduction of the gain for input biases above threshold (bias=1) is also observed. Overall, one observes that the threshold nonlinearity is linearized. This linearization of the $f$–$I$ curve is due to noise-induced firing in the network; for neurons operating in the subthreshold regime, noise allows them to reach threshold, where they would not in the absence of noise. For neurons in the superthreshold regime the noise allows them (on average) to reach threshold slightly quicker than they would without input fluctuations. As more noise is added to the deterministic LIF network the neurons are able to fire with lower levels of input bias. This effectively linearizes the $f$–$I$ curve and increases the overall activity of the network.

### 3.2 Feedback-induced gain control in deterministic networks

Next, simulations without noise but with feedback were done to show that feedback alone can linearize $f$–$I$ curves. This linearization due to feedback is, as we will see, related to the result of Ermentrout (1998) in the context of adaptation. Inhibitory feedback linearizes the $f$–$I$ curve, as seen in Fig. 4. The top curve (solid line) shows the standard $f$–$I$ curve for a deterministic LIF network without feedback. As inhibitory feedback strength is increased, the $f$–$I$ curve divisively shifts downward, breaking off from the $g = 0$ curve at lower values of the bias. Qualitatively one can say that, with increasing inhibitory feedback, the $f$–$I$ curve acquires an increased curvature right near rheobase (near the break-off point), but less curvature (i.e. more linearity) over a broader range thereafter in comparison to the open loop curve. The curves are nevertheless still not straight, being overall downward concave, due in particular to the refractory period which limits the rate. Further, at stronger feedback, the curves are seen to acquire a wavy character, which relates to phase locking (see below).

To understand the mechanism behind the divisive gain shift in Fig. 4, we first look at network raster plots and voltage traces for various feedback strengths and input biases. Comparing Figs. 5b and a and 6b and a, we see that stronger inhibitory feedback reduces the firing rate. This is due to the hyperpolarizing effect of the delayed inhibitory spikes on the membrane potential of the neurons in the network. The decrease in membrane potential delays the next firing time of the neurons (as long as the delay, $\tau_d$, is not too large). In other words, the inhibition causes the membrane potential to take longer to reach threshold. For stronger inhibitory feedback, neurons fire at even later times, and thus as inhibitory feedback strength is increased, the firing rate of the network decreases further still.

In fact, the decrease is in proportion to the amount of firing that would occur in the network without feedback. Thus the $f$–$I$ curves acquire a decreased slope, i.e. exhibit a divisive effect, rather than become shifted to the right as for a subtractive effect. In other words, the inhibition is less effective for a low input bias compared to a high input bias, due to the fact that the feedback is a function of firing rate which

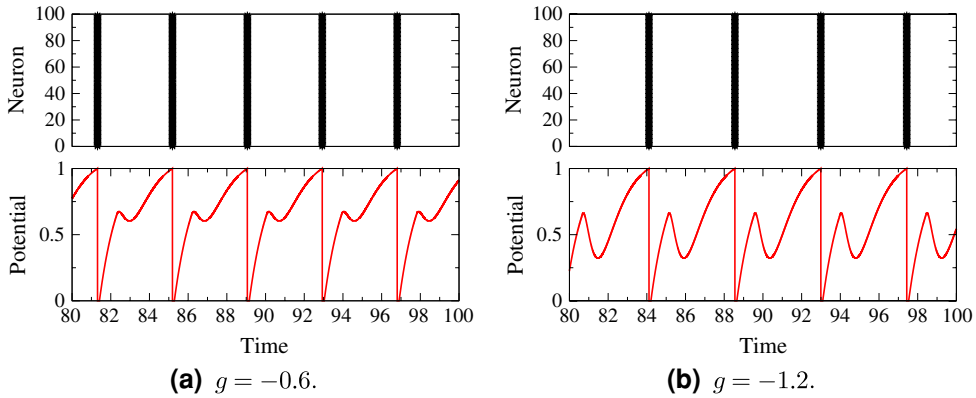


**(a)** $g = -0.6$. **(b)** $g = -1.2$.

**Fig. 5** Network raster plot and single cell voltage curve for $\mu = 1.1$ for two strengths of negative feedback (*left panel* $g = -0.6$, *right panel* $g = -1.2$) and $\alpha = 3$

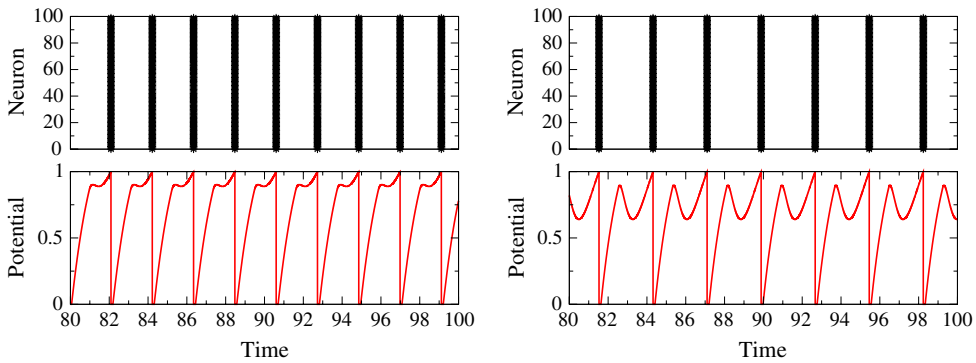


**(a)** $g = -0.6$. **(b)** $g = -1.2$.

**Fig. 6** Network raster plot and single cell voltage curve for $\mu = 1.5$ for two strengths of negative feedback (*left panel* $g = -0.6$, *right panel* $g = -1.2$) and $\alpha = 3$

depends on the input bias. In fact, as the input current is lowered to the rheobase current, the firing becomes increasingly less sensitive to changes in feedback strength, since in that limit the firing rate goes to zero. In contrast, for large inputs an increase in feedback strength can significantly lower the firing rate, due again to the dependence on $\mu$ of the inhibitory current caused by the feedback. The multiplicative effect can also be gauged visually in the time series by comparing the magnitude of the shift in firing rate between Fig. 5b and a, and the shift in firing rate between Fig. 6b and a obtained at a higher bias. These divisive shifts are clearly displayed as an increasing separation between curves in the $f$–$I$ curves of Fig. 4 (see also Fig. 8).

Figure 4 also shows that the smoothness of the $f$–$I$ curve disappears when inhibitory feedback is present in the network (i.e. there are small bumps seen in the $f$–$I$ curves with inhibitory feedback). This is not caused by fluctuations due to noise, since there is no noise here (Perkel et al. 1964). As the input bias is increased for a constant, nonzero feedback strength, the depolarization of the membrane occurs quicker and the inhibitory feedback affects it at a later stage in its rise time and with a smaller amplitude (compare Figs. 5b and 6b). If the input bias is large enough, the neuron may even fire before the inhibitory feedback has a chance to affect it, due to the time delay of the feedback $\tau_d$ (Fig. 7b). This causes different firing patterns for different input bias strengths. For input bias values near the transition from one firing pattern (Fig. 6b) to the next (Fig. 7b) the in-step phase locking of neurons in the network becomes destabilized as in Fig. 7a. As we will use the same simulation time to compute mean firing rate (see next subsection), and this span of time does not contain an integer number of periods of the solution regardless of the parameters, the $f$–$I$ curves for such noiseless inhibitory feedback dynamics are not smooth like the no-feedback case. This effect is however small compared to the abrupt jumps caused by transitions between different firing patterns.

### 3.3 The combined effects of fluctuations and feedback on gain control

Introducing noise into a network with inhibitory feedback further linearizes the $f$–$I$ curve and smoothes out this bumpiness. Figure 8 shows a comparison of a completely deterministic network and three stochastic networks with varying levels of noise. The divisive shift in the gain due to feedback that is seen in the deterministic network (Fig. 8a) is also present in Fig. 8b, c, d, which have both feedback and noise. The curves in each plot further seem to connect up at low rates, i.e. the behavior due to inhibition caused by self-feedback is

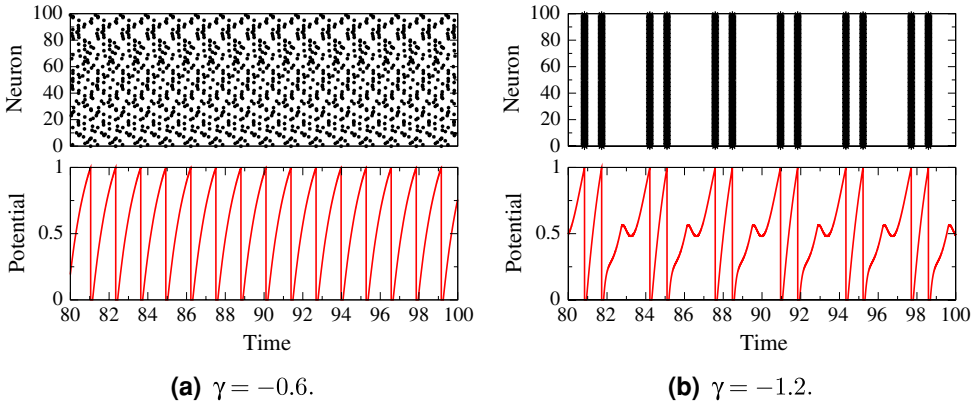


**Fig. 7** Network raster plot and single cell voltage curve for $\mu = 1.9$ for two strengths of negative feedback (*left panel* $g = -0.6$, *right panel* $g = -1.2$) and $\alpha = 3$

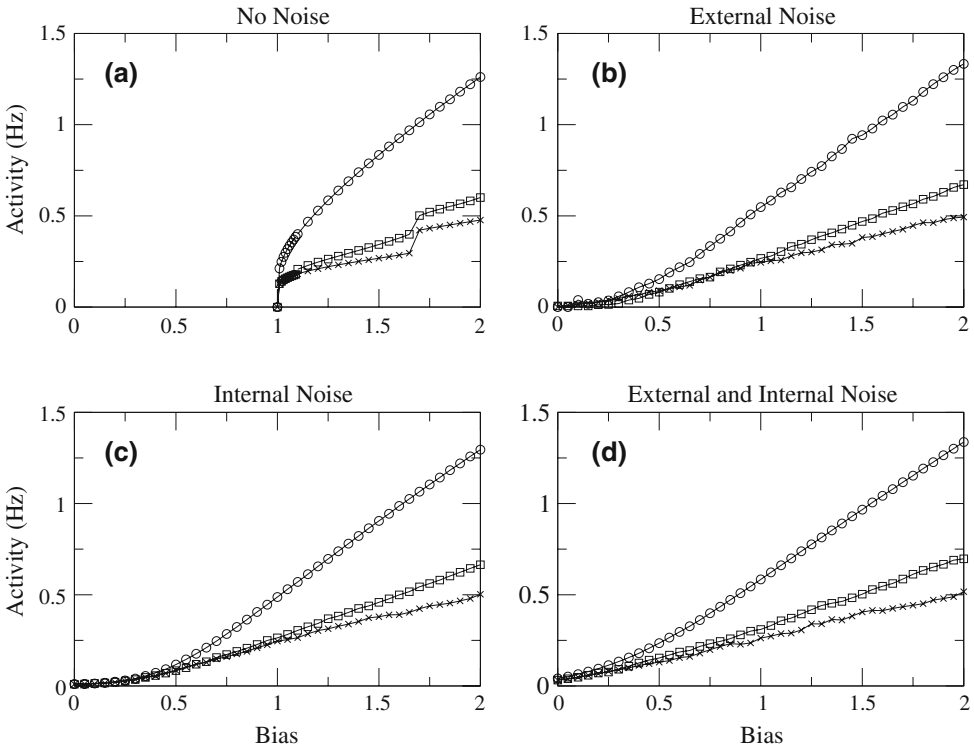


**Fig. 8** $f$–$I$ curves with increasing inhibitory feedback strength for **a** a network with no noise, **b** a network with global external noise, **c** a network with internal noise and **d** a network with both internal and global external noise. Parameters are the same as those in Fig. 3. As the strength of inhibitory feedback is increased, the curves divisively shift down, without and with noise. Linearization of the $f$–$I$ curves, especially near and below threshold, is also seen in the transition from **a** to **d** as more noise is added. *Circles* feedback gain $g = 0$, *squares* $g = -1.2$, and *crosses* $g = -2.4$. Noise intensities are as in Fig. 3, and $\alpha = 2$

divisive rather than subtractive. Interestingly, in going from no feedback and no noise to a feedback and noise situation, there is both a slope change and a leftward shift which may be seen in some experimental situations.

The addition of noise smoothes out the $f$–$I$ curve (e.g. the phase locking bumps) and linearizes it notably in the subthreshold regime as seen in Fig. 3. It is also apparent from Fig. 8b, c, and d that, while the noise linearizes the $f$–$I$ curve in the subthreshold regime, it also allows linearization due to feedback in this regime, which is not possible in Fig. 8a because the deterministic network does not fire below threshold.

The combination of the two linearizing effects of noise and feedback could possibly produce a gain shift similar to the one seen in the weakly electric fish (Bastian 1986) and in rat cortex (Chance et al. 2002) for unbalanced inhibition and excitation. These experimental studies showed not only a divisive gain shift, but a subtractive gain shift as well (a small effect in the case of Bastian 1986). Figure 9 shows an overlay of the solid line of Fig. 8a and the dashed line of Fig. 8d. It is clear from the overlay that the combination of the two linearization effects, starting from a situation without noise and feedback, can produce a leftward shift and a multiplicative decrease in the gain. The feedback produces the divisive shift in the gain, with the onset of firing always occurring at the same point since feedback effects require a non-zero firing rate. The increase of noise shifts the initial firing point to a lower input bias level, causing the subtractive shift in the gain. If for some reason the noise decreased, the shift would be to the right. Thus, the model predicts that

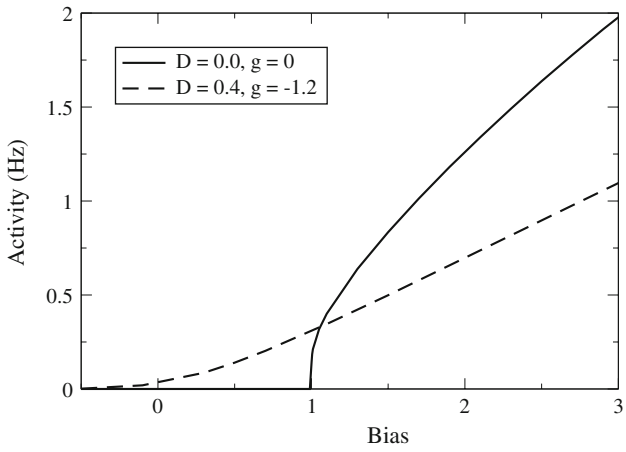


**Fig. 9** $f$–$I$ curve for a cell in the network with no feedback and no noise, *solid line* compared to the $f$–$I$ curve for a network with feedback ($g = -1.2$) and noise ($D = 0.16$)

tuned variations of feedback gain and noise level can produce a variety of effects seen upon manipulating feedback loops.

## 4 Theory

For a stochastic LIF neural network with feedback the mean firing rate can be calculated using the system of implicit equations (Doiron et al. 2004):

$$r = \left[\tau_R + \sqrt{\pi}\int_b^a \mathrm{e}^{x^2}\mathrm{erfc(x)dx}\right]^{-1} \tag{5}$$

where

$$a = \frac{\mu_{\mathrm{eff}} - \Theta}{\sqrt{2D}}, \tag{6}$$

$$b = \frac{\mu_{\mathrm{eff}}}{\sqrt{2D}}, \tag{7}$$

and

$$\mu_{\mathrm{eff}} = \mu + gr(\mu_{\mathrm{eff}}). \tag{8}$$

The feedback strength $g$ in the last equation can be interpreted as taking into account the number of cells in the network, i.e. it scales as $1/N$ (but we keep $N$ fixed throughout our study). The top equation is the expression for the mean firing rate of any current based LIF model with additive Gaussian white noise and drift $\mu_{\mathrm{eff}}$. This drift is however a corrected version of the open loop drift $\mu$ since feedback spikes produce a mean current of $gr$. Together these equations must be solved self-consistently, i.e. using a root finding algorithm.

To calculate how gain depends on the strength of feedback we take the derivative of the mean firing rate with respect to the input bias. Differentiating Eq. (5) with respect to $\mu$ we obtain

$$\frac{\mathrm{d}r}{\mathrm{d}\mu} = \frac{\partial r}{\partial \mu_{\mathrm{eff}}}\frac{\partial \mu_{\mathrm{eff}}}{\partial \mu} \tag{9}$$

where

$$\frac{\partial \mu_{\mathrm{eff}}}{\partial \mu} = 1 + g\frac{\mathrm{d}r}{\mathrm{d}\mu}. \tag{10}$$

Substituting Eq. (10) back into Eq. (9) we get

$$\frac{\mathrm{d}r}{\mathrm{d}\mu} = \frac{\partial r}{\partial \mu_{\mathrm{eff}}}\left(1 + g\frac{\mathrm{d}r}{\mathrm{d}\mu}\right). \tag{11}$$

Rearranging we obtain

$$\frac{\mathrm{d}r}{\mathrm{d}\mu} = \frac{\frac{\partial r}{\partial \mu_{\mathrm{eff}}}}{1 - g\frac{\partial r}{\partial \mu_{\mathrm{eff}}}}. \tag{12}$$

On the other hand,

$$\frac{\partial r}{\partial \mu_{\mathrm{eff}}}(\mu_{\mathrm{eff}}) = r^2\sqrt{\frac{\pi}{2D}}\left[e^{a^2}\mathrm{erfc(a)} - \mathrm{e}^{b^2}\mathrm{erfc(b)}\right]. \tag{13}$$

We note that this is exactly $\frac{\mathrm{d}r}{\mathrm{d}\mu}(\mu)$ for a stochastic network without feedback, for which the open loop mean rate is:

$$r = \left[\tau_R + \sqrt{\pi}\int_b^a \mathrm{e}^{x^2}\mathrm{erfc(x)dx}\right]^{-1} \tag{14}$$

where

$$a = \frac{\mu - \Theta}{\sqrt{2D}}, \tag{15}$$

$$b = \frac{\mu}{\sqrt{2D}}. \tag{16}$$

This means that the following holds:

$$\frac{\partial r(g)}{\partial \mu_{\mathrm{eff}}} = \frac{\mathrm{d}r(g=0)}{\mathrm{d}\mu} \tag{17}$$

i.e. $\frac{\partial r}{\partial \mu_{\mathrm{eff}}}$ is equal to the open loop (no feedback) slope $\frac{\mathrm{d}r(g=0)}{\mathrm{d}\mu}$. By looking at the curve for $g = 0$ in Fig. 10 we see that the slope is approximately constant for a sufficiently small range of $\mu$. This will depend on the total noise intensity, $D$, of the system, which also affects the firing rate. In this case, $D = 0.16$ and $0.3 < \mu < 5.0$ is sufficient.

For an approximately constant slope $\frac{\mathrm{d}r(g=0)}{\mathrm{d}\mu} \equiv \gamma$, which is a positive constant, Eq. (12) becomes

$$\frac{\mathrm{d}r(g)}{\mathrm{d}\mu} \simeq \frac{\gamma}{1 - g\gamma}. \tag{18}$$

Integrating this relation with respect to $\mu$ yields

$$r(g) \simeq \frac{\gamma}{1 - g\gamma}\mu + C \tag{19}$$

where $C$ is the constant of integration. Equation 19 reveals that inhibitory feedback ($g < 0$) divisively reduces the positive slope of the $f$–$I$ curve, similarly to the effect of

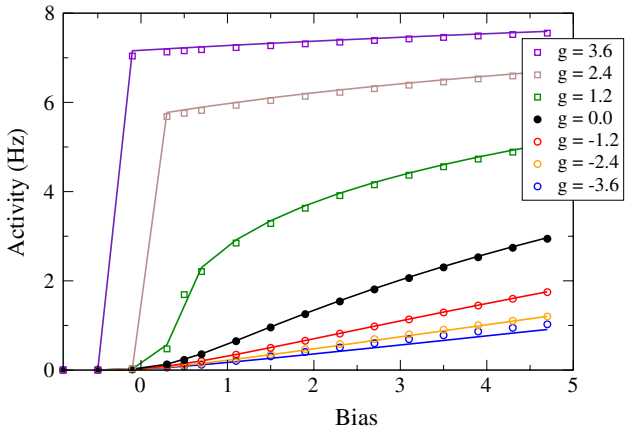


**Fig. 10** Mean firing rate of a cell in the network as a function of the input bias ($\mu$) for various inhibitory (*open circles*) and excitatory (*open squares*) feedback strengths. The *solid circles* represents the activity of a network with no feedback. Parameters used for these simulations were $\sigma^2 = 0.16$. The theoretical (*solid lines*) activity of the network, Eq. (5), matches numerical simulations (*symbols*) very well. Here $\alpha = 3$

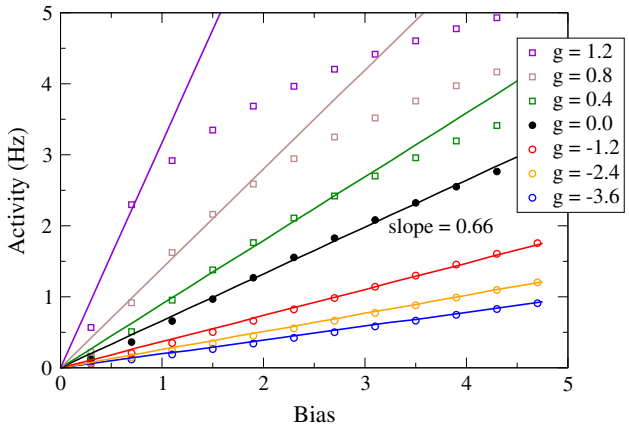


**Fig. 11** Mean firing rate on a cell in the network as a function of the input bias ($\mu$) for various inhibitory (*open circles*) and excitatory (*open squares*) feedback strengths. The solid circles represent the activity of a network with no feedback. Parameters used for these simulations were $\sigma^2 = 0.16$ and $D_{\text{int}} = 0$. The theoretical linear approximation to the network activity Eq. (19) (*solid lines*) matches numerical simulations (*symbols*) for inhibitory feedback, and for a small range of biases around threshold for excitatory feedback. Here $\alpha = 3$

deterministic adaptation studied in Ermentrout (1998). The reduction is proportional to $|g|$. For positive feedback, this equation further predicts a divisive increase in the positive slope of the $f$–$I$ curve as $g$ increases.

## 5 Comparison of theory and simulations

### 5.1 $f$–$I$ curves for positive or negative feedback

So far we have looked at inhibitory feedback, but as we will see below, excitatory feedback also divides the gain of the $f$–$I$ curves. Thus in this Section, we compare theory and simulation results separately for inhibitory and excitatory feedback.

Figure 10 shows the network activity as a function of input current bias ($\mu$) for excitatory and inhibitory feedback in our stochastic LIF neural network. Agreement between the network simulations and the rates estimated from the self-consistent equations is very good for a wide range of inhibitory feedback strengths. Looking at the $f$–$I$ curves for $g = -2.4$ and $g = -3.6$ in Fig. 10, we see that increasing already strong inhibitory feedback only elicits a small divisive decrease in the gain. This indicates a limitation of the network to modify its firing frequency for extremely strong inhibitory feedback.

Increasing excitatory feedback causes the activity of the network to increase as compared to the zero feedback case. The $f$–$I$ curve near the onset of firing shows a divisive increase in the gain for increasing excitatory feedback. Interestingly, for larger input bias values, the gain divisively increases for weak excitatory feedback, but divisively decreases for strong excitatory feedback (compare the slope of the two top curves at higher biases). A further increase of excitatory feedback strength or input bias has less effect at such extreme high firing rates. All of these effects are accurately predicted by theory (Eq. 5), as the theoretical results match well with simulation results in Fig. 10.

The linear approximation, Eq. (19), also predicts simulation results for values of input bias larger than approximately 0.3. For $\gamma < 1 - g\gamma$ the slope of the $f$–$I$ curve will be small and positive. This occurs for all negative values of $g$ as seen in Fig. 10 for all values of $\mu$. More rigorously we compare simulation data to Eq. (19) in Fig. 11 and see that indeed the approximation is good for inhibitory feedback for all values of input bias.

For $\gamma > 1 - g\gamma$ the slope of the $f$–$I$ curve will be positive and larger than the open loop slope for the stochastic network. This occurs for a small range of positive $g$ values for certain values of $\mu$—see Fig. 10 for $g = 1.2$. The expanded range in Fig. 11 reveals that Eq. (19) indeed matches simulation results for small positive feedback only for intermediate values of input bias.

An interesting effect, which is not accounted for by the linear approximation, is the decrease of the slope for large positive values of $g$, as seen in the top two curves of Fig. 10. The network here exhibits bistability, a nonlinear effect, and jumps to its higher rate (Laing and Longtin 2003). At such large rate values, the open-loop slope $\gamma$ tends toward zero, due to the saturation caused by the absolute refractory period; thus, regardless of $g$, the slope of the $f$–$I$ curve is approximately zero as seen from the top two curves of Fig. 10. A larger value of $g$ brings on the saturation even earlier, and consequently, the slope is slightly smaller.

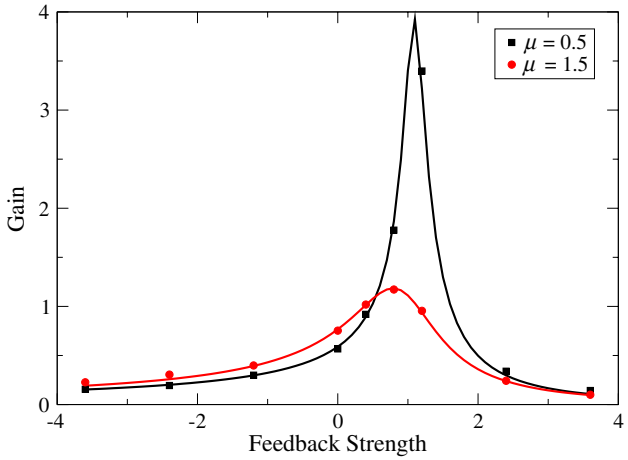


**Fig. 12** The gain (slope of the $f$–$I$ curves) of a given cell in the network plotted against feedback strength, $g$, for two different values of input bias, $\mu$. The black squares and red circles represent simulation data for $\mu = 0.5$ and $\mu = 1.5$ respectively. The slope was calculated using two simulated points on the $f$–$I$ curve close to $\mu = 0.5$ and $\mu = 1.5$, for various g. The parameters used for these simulations are the same as in Fig. 10. The *solid lines* represent theoretical results obtained from Eq. (12), which agree very well with simulation results. Noise intensities are as in Fig. 3. Here $\alpha = 3$

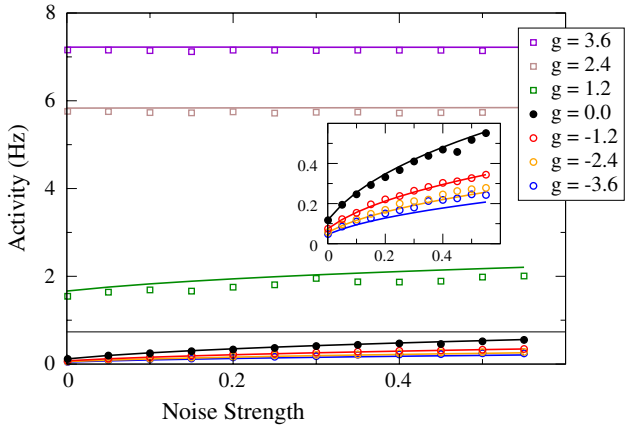


**Fig. 13** Firing activity of one cell in the network as a function of input noise strength ($\sigma$), which represents the stimulus contrast, for various amounts of inhibitory (*open circles*) or excitatory (*open squares*) feedback. The *solid circles* represents the activity with no feedback. Parameters used for these simulations are as in Fig. 10 with $\mu = 0.5$. The theoretical activity of the network (solid lines), Eq. (5), matches numerical simulations (*symbols*) very well. Here $\alpha = 3$

In summary, the linear theoretical approximation predicts simulation results for values of $\mu$ around 1, i.e. around the threshold value in the absence of noise. There, the slope of the $f$–$I$ curve increases as $g$ goes from negative to small positive values. And for positive $g$ values, the agreement is limited to a narrower range as $g$ becomes larger.

If we return to the full solution of the self-consistent rate equation, we find that we can accurately predict theoretical values of firing rates and the slope of $f$–$I$ curves for a wide range of feedback strengths, as shown in Fig. 12. In particular, the decrease in gain for stronger positive feedback is seen clearly on the curves.

### 5.2 Mean firing rate versus stimulus contrast

Separating the external input into a time-dependent and time-independent part allows us to look at the effect of the external noise intensity on the activity of the network independent of the average external input (input bias). This amounts to looking at the effect of stimulus contrast around a given stimulus mean, assuming here that the stimulus is a Gaussian white noise, for simplicity. The activity of the network for a constant input bias and increasing signal (stimulus) noise strength, as seen in Fig. 13, behaves similarly to that found for increasing input bias and constant noise strength, which had been our focus up to know. As the signal noise strength increases, so does the activity of the network. Increasing the inhibitory feedback strength of the network lowers the overall activity in a divisive manner, as before. Increasing the positive feedback strength of the network increases the network activity in a divisive manner (not shown - this is true increasing $g$ from 0 to 1.2, but this is not quite visible in Fig. 13). Figure 13 further shows that, for increasing inhibitory feedback strength at already large negative values of g, the network is less and less able to change its rate. And at large positive values of $g$, increasing signal noise strength has even less effect on the network activity. Theoretical network activity is also plotted in Fig. 13 to show again that Eq. 5 predicts the activity of the network fairly well.

In summary, for a network with low activity, increasing the input noise strength increases the activity of the network (see inset of Fig. 13), but networks with high activity and/or large feedback strengths are virtually unaffected by increasing the input noise strength. These results agree with those found in Doiron et al. (2001) and Burkitt et al. (2003).

## 6 Discussion

We have presented a theoretical and numerical analysis of the influence of additive (i.e. current) spike-based delayed feedback on gain control. The study was motivated by electrosensory neurons that receive stimulus input (via receptor cells) and as well as feedback input from higher brain centers. This is a common set-up for many other sensory pathways, including thalamo-cortical and cortico–cortico systems. Modeling feedback as a current input is a good approximation when the feedback arrives at dendritic sites, and the spiking is decided at the hillock (Koch 1999). We have shown that negative spiking feedback in the network of stochastic LIF neurons leads to a decrease in slope of the $f$–$I$ curve without changing

its threshold, and is thus a purely divisive effect. In contrast, positive feedback increases the slope, and could be labeled as a purely multiplicative effect since the gain increases. Nevertheless, we feel that it is perhaps best to keep a commonly accepted label of "division" for both these effects, which are in fact pure "scaling" effects. When sufficiently strong, positive feedback leads to a jump to higher firing rates; such a jump, which is caused by bistability, is not seen in the negative feedback case.

The divisive control is seen from zero to large firing frequencies, as opposed to the noise-induced divisive control in open-loop which occurred at lower rates in Doiron et al. (2001). By itself, the feedback linearizes the $f$–$I$ curve in a manner described by Ermentrout (1998) in the context of spike frequency adaptation, or by Douglas et al. (1995) in the context of contrast invariance using recurrent nets. Our addition of noise extends this linearization well into the subthreshold domain, whether this noise is intrinsic to the cell or from external input. The combination of the noise and feedback results in an important linearization and divisive behavior without a concomitant threshold shift, i.e. without a subtractive gain control. This is in contrast to recently proposed noise-based divisive gain control (Doiron et al. 2001) in which there is also a threshold change unless a balanced of excitation and inhibition is somehow carefully maintained (Chance et al. 2002).

The feedback delay, included in our study for generality, does not affect the results significantly except for the emergence of oscillations in the presence of moderate to strong negative feedback. This leads to a sequence of different phase locking patterns as the bias current increases. This finer structure of the $f$–$I$ curve disappears progressively as the level of noise increases, as expected from open-loop studies (French et al. 1972). Most of our results were obtained for the classic $f$–$I$ curves. But we also considered mean firing frequency-versus-stimulus contrast, the latter being defined as the standard deviation of a band-limited noisy modulation around a fixed bias. We found that divisive effects occur also in this case, which is relevant when certain stimuli leave the mean depolarization of a cell unchanged, as has recently been observed in primary visual cortex in response to spatially broadband stimuli (Cardin et al. 2008).

The self-consistent rate equation for the recurrent network of stochastic LIF neurons has been solved numerically at different values of the bias to obtain $f$–$I$ curves. The predictions agree well with numerical simulations of the network activity. Further we have developed a theory for the dependence of the gain on the parameters of the problem, including the feedback gain and noise level. It yields good agreement with the numerical simulations. It also extends to the positive feedback case, and explains certain features of the $f$–$I$ curves even near the saturation regime imposed by the refractory period.

The self-consistent rate equation used to calculate the closed loop $f$–$I$ curves was posited only for the mean rate. This is simply a balance that takes into account the effect of the mean of the feedback on the bias of the cell, with the result that one of the cells in closed loop fires at a rate given by its open loop characteristic but with a corrected or "effective" bias. This effective bias is higher (lower) than the open-loop bias when positive (negative) feedback is present. Note however that the feedback input is also an extra source of noise for the single cells, and in principle one may wish to write a second self-consistent equation—coupled to the first—for the variance of the rate. Given that our results are fairly accurate using only a self-consistent equation for the rate, this suggests that the extra noise variance contributed by the feedback is not significant. This can be understood from two considerations.

First, at low rates, there is little current being fed back, and thus its variance is also small. So the effect is basically one of linearization by feedback as described by Ermentrout (1998) and extended here to the stochastic context (apart from the delay effects). At higher rates, the variance may be higher, but the $f$–$I$ curves are less sensitive to increases in noise as Fig. 3 reveals. This is a form of noise suppression, however the context here is internal and/or input (external) noise, as opposed to external noise with deterministic neurons as in Douglas et al. (1995). The second consideration is the averaging that occurs in the network, due to the $1/N$ factor in the feedback coupling. The standard deviation of the total feedback current is proportional to $\sqrt{N}$ times the standard deviation of the current contributed by one cell. Dividing by $N$ yields a relatively lower fluctuation in comparison to the mean rate (see also Chacron et al. 2005).

Our results on divisive control offer a possible explanation for the observation of an increase in slope of the $f$–$I$ curve in the weakly electric fish (Bastian 1986), which is the main effect of opening an important feedback loop. Insofar as the main effect of opening the feedback is a slope change, our study suggests how this can occur. However, if there is a concomitant shift of rheobase, then a change in noise along with the feedback can account for that, as seen in going from the solid line in Fig. 8a to the dashed line in Fig. 8d. The increased feedback alone is clearly not able to account for both slope change and a significant subtractive shift, even though feedback spikes contribute some noise (which is taken account by the simulation).

Related work (Mehaffey et al. 2005) in an in vitro preparation of the ELL has shown how inhibition targeting the proximal apical dendrite of ELL pyramidal cells can also replicate the in vivo results (Bastian 1986). In that study the active dendrite of the ELL pyramidal cell acted as a source of positive feedback on the cell's soma, and in an analogous way to the results presented here, increased the slope of the static transfer curve. Inhibition from descending pathways reduced

the total dendro-somatic current, which resulted in an overall reduction of the positive feedback and caused a decrease in the $f$–$I$ curve slope. From a biophysical perspective there are significant differences between the electrosensory gain control scheme presented here and the one in Mehaffey et al. (2005), however, the overall conclusions on how feedback influences the static transfer gain of spiking neurons are very similar. To our knowledge, there is no reason as to why these gain control schemes could not be both active during electrosensing, increasing the overall range of gain modulation in the electrosensory system.

The work also extends the gain control model of Nelson (1994) which can be considered a first approximation to the gain control problem. In that approach, the neuron transmembrane potential was the quantity fed back to itself, rather than the firing rate. It would be interesting to extend our work here to the specific context of simultaneous positive and negative feedback loops that he studied, although the inclusion of reversal potentials for both positive and negative feedback pathways would seriously complicate the theoretical analysis. Nevertheless, we expect the divisive effects discussed here to simply compete with one another. It is also worth considering the effect of simultaneous positive and negative delayed feedback on gain control, in which scaling may occur on top of a mixture of chaotic and stochastic network dynamics (Laing and Longtin 2003).

Relatedly, the feedback synaptic input used in our work acts additively on the current balance equation. It is on equal footing with the individual internal noise source for each cell, and with external input from e.g. external stimuli. In the inhibitory case, it is only an approximation to shunting inhibition which, by definition, involves a synapse with reversal potential near the resting potential and thus acts most strongly when the inhibitory input drives the cell in the vicinity of resting potential. We have verified (not shown) that the numerical results found here for additive "current-based" feedback also hold for the case of conductance-based feedback. Thus, divisive behavior is seen for either feedback shunting inhibition or for excitatory synaptic feedback, either with internal noise or without. This extends the results in Douglas et al. (1995) to the case where the cells have internal noise. A theoretical analysis of such conductance-based feedback is more involved than the additive noise case and will be left for future work.

We have chosen the feedback strength $g$ and the intensity of the noises $\sigma$ and $D_{int}$ as control parameters; the specific values chosen are consistent with past studies (Doiron et al. 2004, 2003). A full parametric study with $\alpha$ and $\tau$ for different values of feedback gain and noise is beyond the scope of our study. Nevertheless we have performed preliminary simulations for values of $\alpha$ ranging from 0.2 to 20 in the presence of internal noise ($D_{int} = 0.08$) and $g = -1.2$. For $0.2 < \alpha < 10$ the results are statistically the same as those for $\alpha = 2$, but begin deviating for larger values of $\alpha$, i.e. for much faster synaptic kinetics (not shown). For example, for $\alpha = 20$, divisive gain control is still observed, but the feedback is less effective, corresponding to firing rates about 20% higher than for $\alpha = 2$. The systematic exploration of these effects is left for future studies, but divisive behavior is nevertheless insensitive to large variations in $\alpha$, in agreement with our theory.

While we have limited our analysis to a network of LIF models with additive feedback, other single cell spiking dynamics could be considered. From a theoretical standpoint, one could use the firing function that best fits experimental data. For example, Type I dynamics may underlie firing in open loop; in this case the analytic modeling could proceed using mean firing rate formulae developed for the stochastic quadratic integrate-and-fire model (Lindner et al. 2003). And in the absence of a good theory for the open loop $f$–$I$ curve, a numerical interpolating fit to the experimental $f$–$I$ curve could be used in the self-consistent rate equation that needs to be solved (numerically) to obtain the steady state firing rate.

Our approach can be extended to networks involving sub-populations of cells with different strengths and polarities of feedback amongst them. In this case one would likely see a combination of the effects reported here. The analytic work would then involve writing and solving a self-consistent set of equations to obtain the effective biases of each population and their associated $f$–$I$ curves.

We expect that including adaptation currents explicitly would enhance linearization of the $f$–$I$ curves and support the divisive behavior further, although in the presence of noise it will render the analytic modeling more challenging. And eventually one would like to understand the gain control for inputs that are not slow, a venture that would require importing linear response functions calculated using Fokker–Planck theory. In particular it would be interesting to compute the response time of the network with spiking feedback, and compare to rate model descriptions in which this time is known to vary with recurrent feedback, sometimes unfavorably due to critical slowing down near instabilities brought on by negative feedback (Chance and Abbott 2000).

Finally, feedback pathways are known to exhibit varying forms of plasticity. It is known for example that the cerebellar EGP feedback pathway to the ELL pyramidal cells, that was impaired in the motivating study of Bastian (1986), exhibits anti-Hebbian plasticity designed to cancel redundant inputs (Bastian et al. 2004), as it does in mormyryd electric fish (Grant et al. 1996; Bell et al. 1997). Other feedback pathways in the electric fish are known to involve a mixture of short-term facilitation and depression. The feedforward pathway to cells in the ELL further involve a mostly depressing synapse (Len Maler, personal communication). Future work will aim to figure out the role that such plastic feedforward

and feedback connections play in the regulation of gain over a range of time scales in the input.

**Acknowledgments** This work was supported by NSERC Canada (A.L.) and the Human Frontiers Science Program (B.D.).

## References


Alitto HJ, Usrey WM (2004) Influence of contrast on orientation and temporal frequency tuning in ferret primary visual cortex. J Neurophysiol 91:2797–2808

Andersen RA, Mountcastle VB (1983) The influence of the angle of gaze upon the excitability of the light-sensitive neurons of the posterior parietal cortex. J Neurosci 3:532–48

Anderson JS, Lampl I, Gillespie DC, Ferster D (2000) The contribution of noise to contrast invariance of orientation tuning in cat visual cortex. Science 290:1968–1972

Arevian AC, Kapoor V, Urban NN (2007) Activity-dependent gating of lateral inhibition in the mouse olfactory bulb. Nat Neurosci 11: 80–87

Arsiero M, Luscher HR, Lundstrom BN, Giugliano M (2007) The impact of input fluctuations on the frequency–current relationships of layer 5 pyramidal neurons in the rat medial prefrontal cortex. J Neurosci 27:3274–3284

Bacci A, Huguenard JR, Prince DA (2003) Functional autaptic neurotransmission in fast-spiking interneurons: a novel form of feedback inhibition in the neocortex. J Neurosci 23:859–866

Baca SM, Marin-Burgin A, Wagenaar DA, Kristan WB (2008) Widespread inhibition proportional to excitation controls the gain of a leech behavioral circuit. Neuron 57:276–289

Bastian J (1986) Gain control in the electrosensory system mediated by descending inputs to the electrosensory lateral line lobe. J Neurosci 6:553–562

Bastian J, Chacron MJ, Maler L (2004) Plastic and non-plastic pyramidal cells perform unique roles in a network capable of adaptive redundancy reduction. Neuron 41:767–779

Bell CC, Han V, Sugawara Y, Grant K (1997) Synaptic plasticity in a cerebellum-like structure depends on temporal order. Nature 387:278–281

Berman NJ, Maler L (1999) Neural architecture of the electrosensory lateral line lobe: adaptations for coincidence detection, a sensory searchlight and frequency-dependent adaptive filtering. J Exp Biol 202:243–1253

Brandt SF, Wessel R (2007) Winner-take-all selection in a neural system with delayed feedback. Biol Cybern 97:221–228

Brown DA, Adams PR (1980) Muscarinic supression of a novel voltagesensitive K+ current in a vertebrate neuron. Nature 183:673–676

Burkitt AN, Meffin H, Grayden DB (2003) Study of neuronal gain in conductance-based leaky integrate and fire neuron model with balanced excitatory and inhibitory synaptic input. Biol Cybern 89:119–125

Carandini M, Heeger DJ (1994) Summation and division by neurons in primate visual cortex. Science 264:1333–1336

Cardin JA, Palmer LA, Contreras D (2008) Cellular mechanisms underlying stimulus-dependent gain modulation in primary visual cortex neurons in vivo. Neuron 59:150–160

Chacron MJ, Longtin A, Maler L (2005) Delayed excitatory and inhibitory feedback shape neural information transmission. Phys Rev E 72:051917

Chance FS, Abbott LF (2000) Divisive inhibition in recurrent networks. Netw Comput Neural Syst 11:119–129

Chance FS, Abbott LF, Reyes AD (2002) Gain modulation from background synaptic input. Neuron 35:773–782

Diez-Martinez O, Segundo JP (1983) Behaviour of a single neuron in a recurrent excitatory loop. Biol Cybern 47:33–41

Doiron B, Longtin A, Berman N, Maler L (2001) Subtractive and divisive inhibition: effect of voltage-dependent inhibitory conductances and noise. Neural Comput 13:227–248

Doiron B, Chacron MJ, Maler L, Longtin A, Bastian J (2003) Inhibitory feedback required for network oscillatory responses to communication but not prey stimuli. Nature 421:539–543

Doiron B, Lindner B, Longtin A, Maler L, Bastian J (2004) Oscillatory activity in electrosensory neurons increases with the spatial correlation of the stochastic input stimulus. Phys Rev Lett 93:048101

Douglas RJ, Koch C, Mahowald M, Martin KAC, van Vreeswijk C (1995) Recurrent excitation in neocortical circuits. Science 269:981–985

Ermentrout GB (1998) Linearization of $F$–$I$ curves by adaptation. Neural Comput 10:1721–1729

Ferster D, Miller KD (2000) Neural mechanisms of orientation selectivity in the visual cortex. Ann Rev Neurosci 23:441–471

French AS, Holden AV, Stein RB (1972) The estimation of the frequency response function of a mechanoreceptor. Kybernetik 11:15–23

Gabbiani F, Krapp HG, Koch C, Laurent G (2002) Multiplicative computation in a visual neuron sensitive to looming. Nature 420:320–324

Grant K, Bell CC, Han V (1996) Sensory expectations and anti-Hebbian synaptic plasticity in cerebellum-like structures. J. Physiol. (Paris) 90:233–237

Hansel D, van Vreeswijk C (2002) How noise contributes to contrast invariance of orientation tuning in cat visual cortex. J Neurosci 22:5118–5128

Higgs M, Slee SJ, Spain WJ (2007) Diversity of gain modulation by noise in neocortical neurons: regulation by the slow afterhyperpolarization conductance. J Neurosci 26:8787–8799

Holt GR, Koch C (1997) Shunting inhibition does not have a divisive effect on firing rates. Neural Comput 9:1001–1013

Knight BW (1972) Dynamics of encoding in a population of neurons. J Gen Physiol 59:734–766

Koch C (1999) Biophysics of computation. Oxford University Press, New York

Larkum ME, Senn W, Luscher HR (2004) Top-down dendritic input increases the gain of layer 5 pyramidal neurons. Cereb Cortex 14:1059–1070

Laing CR, Longtin A (2003) Dynamics of deterministic and stochastic paired excitatory-inhibitory delayed feedback. Neural Comput 15:2779–2822

Le Masson G, Renaud-Le Masson, Debay D, Bal T (2002) Feedback inhibition controls spike transfer in hybrid thalamic circuits. Nature 417:854–858

Lindner B, Longtin A, Bulsara AR (2003) Analytical expressions for rate and CV of a Type I neuron driven by Gaussian white noise. Neural Comput 15:1761–1788

Lindner B, García-Ojalvo J, Neiman A, Schimansky-Geier L (2004) Effects of noise in excitable systems. Phys Rep 392:321–427

Longtin A (1993) Stochastic resonance in neuron models. J Stat Phys 70:309–327

Longtin A (2000) Adiabatic and non-adiabatic resonances in excitable systems. In: Stochastic processes in physics, chemistry and biology. Lecture notes in physics, vol 93. Springer, Berlin, pp 172–181

Longtin A, Doiron B, Bulsara AR (2002) Noise-induced divisive gain control in neuron models. BioSystems 67:147–156

Ly C, Doiron B (2009) Divisive gain modulation with dynamic stimuli in integrate-and-fire neurons. PLoS Comp Biol (in press)

Madison DV, Nicoll RA (1984) Control of the repetitive discharge of rat CA1 pyramidal neurones in vitro. J Physiol 354:319–331

McAdams CJ, Maunsell JHR (1999) Effects of attention on orientation tuning functions of single neurons in macaque cortical area V4. J Neurosci 19:431–441

McAdams CJ, Reid RC (2005) Attention modulates the responses of simple cells in monkey primary visual cortex. J Neurosci 25:11023–11033

Mehaffey WH, Doiron B, Maler L, Turner RW (2005) Deterministic multiplicative gain control with active dendrites. J Neurosci 25:9968–9977

Mitchell SJ, Silver RA (2003) Shunting inhibition modulates neuronal gain during synaptic excitation. Neuron 38:433–445

Nelson ME (1994) A mechanism for neuronal gain control by descending pathways. Neural Comput 6:242–254

Pauluis Q, Baker SN, Olivier E (1999) Emergent oscillations in a realistic network: The role of inhibition and the effect of the spatiotemporal distribution of the input. J Comput Neurosci 6:27–48

Perkel DP, Schulman J, Bullock TH, Moore GP, Segundo JP (1964) Pacemaker neurons: effects of regularly spaced synaptic input. Science 145:61–63

Prescott SA, De Koninck Y (2003) Gain control of firing rate by shunting inhibition: roles of synaptic noise and dendritic saturation. Proc Natl Acad Sci (USA) 100:2076

Salinas E, Abbott LF (1996) A model of multiplicative neural responses in parietal cortex. Proc Natl Acad Sci (USA) 93:11956–11961

Salinas E, Thier P (2000) Gain modulation: a major computation principle of the central nervous system. Neuron 27:15–21

Salinas E, Sejnowski TJ (2001) Gain modulation in the central nervous system: where behavior, neurophysiology, and computation meet. Neuroscientist 7:430–440

Schwabe L, Obermayer K, Angelucci A, Bressloff PC (2006) The role of feedback in shaping the extra-classical receptive field of cortical neurons: a recurrent network model. J Neurosci 26:9117–9129

Segundo JP (1970) Communication and coding by nerve cells. In: Quarton GC, Melnechuk T, Schmitt FO (eds) The neurosciences. Second study program. Rockefeller University Press, New York, pp 569–586

Trotter Y, Celebrini S (1999) Gaze direction controls response gain in primary visual-cortex neurons. Nature 398:239–242

White JA, Chow CC, Ritt J, Soto-Trevino C, Kopell N (1998) Synchronization and oscillatory dynamics in heterogeneous, mutually inhibited neurons. J Comput Neurosci 5:5–16